01 Apr 2018

A Hollow Coaxial Cable Fabry-Perot Resonator for Liquid Dielectric Constant Measurement

Chen Zhu

Yiyang Zhuang

Yizheng Chen

Jie Huang
Missouri University of Science and Technology, jieh@mst.edu

Recommended Citation

C. Zhu et al., "A Hollow Coaxial Cable Fabry-Perot Resonator for Liquid Dielectric Constant Measurement," *Review of Scientific Instruments*, vol. 89, no. 4, American Institute of Physics (AIP), Apr 2018.
The definitive version is available at https://doi.org/10.1063/1.5021684

A hollow coaxial cable Fabry–Pérot resonator for liquid dielectric constant measurement

Chen Zhu, Yiyang Zhuang, Yizheng Chen, and Jie Huang[a)]
Department of Electrical and Computer Engineering, Missouri University of Science and Technology, Rolla, Missouri 65409, USA

(Received 7 January 2018; accepted 25 March 2018; published online 13 April 2018)

We report, for the first time, a low-cost and robust homemade hollow coaxial cable Fabry–Pérot resonator (HCC-FPR) for measuring liquid dielectric constant. In the HCC design, the traditional dielectric insulating layer is replaced by air. A metal disk is welded onto the end of the HCC serving as a highly reflective reflector, and an open cavity is engineered on the HCC. After the open cavity is filled with the liquid analyte (e.g., water), the air-liquid interface acts as a highly reflective reflector due to large impedance mismatch. As a result, an HCC-FPR is formed by the two highly reflective reflectors, i.e., the air-liquid interface and the metal disk. We measured the room temperature dielectric constant for ethanol/water mixtures with different concentrations using this homemade HCC-FPR. Monitoring the evaporation of ethanol in ethanol/water mixtures was also conducted to demonstrate the ability of the sensor for continuously monitoring the change in dielectric constant. The results revealed that the HCC-FPR could be a promising evaporation rate detection platform with high performance. Due to its great advantages, such as high robustness, simple configuration, and ease of fabrication, the novel HCC-FPR based liquid dielectric constant sensor is believed to be of high interest in various fields. *Published by AIP Publishing.* https://doi.org/10.1063/1.5021684

I. INTRODUCTION

Accurate and reliable measurement of the liquid dielectric constant is of great interest and is important in many chemical and biological applications.[1] In the past decades, fiber optic refractive index (RI) sensors have attracted extensive research interest owing to their well-known advantages such as small size, high resolution, high sensitivity, and the multiplexing capability.[2–5] The principle of the most optical fiber based RI sensors is based on the interactions between the evanescent field and external medium of interest. Examples include long-period fiber gratings (LPFGs),[6,7] fiber Bragg gratings (FBGs),[8–10] optical fiber surface plasmon resonance (SPR) sensors,[11,12] bending structure based RI sensors,[13,14] etc. However, the RI response of these sensors (i.e., evanescent field interaction based) is not linear. Therefore, the calibrations of these sensors become cumbersome when quantitative measurements are required. Additionally, these RI sensors are very sensitive to bending which produces unpredictable changes in their characteristic spectra for RI measurements, making it difficult to interpret the sensor signal.

Open cavity based Fabry–Pérot (FP) interferometer has also been widely used for monitoring changes in the RI of liquids and gases. An FP interferometer consists of two reflecting surfaces, which are parallel and separated in space (e.g., tens of microns). An open cavity is engineered on the FP cavity to allow the analyte to fill in. The reflection spectrum of an FP interferometer can be directly affected by the cavity length and the cavity medium refractive index. In comparison with other optical fiber RI sensors (e.g., evanescent field-based sensors), an open cavity based FP refractometer achieves a constant RI sensitivity (i.e., linear response) and covers a wide measurement range. Wei *et al.* reported an all-fiber inline FP interferometer with an open micro-notch cavity fabricated by an fs laser for highly sensitive RI measurement.[15] Tian *et al.* presented a microfluidic FP refractometer using a concave-core photonic crystal fiber.[16] However, the aforementioned FP refractometers are fragile, and their fabrication is costly and complicated. The two reflecting surfaces have to be accurately manufactured to maintain a parallel relationship. These drawbacks seriously hinder their way of practical applications.

A coaxial cable is also a type of waveguide which confines and transmits electromagnetic (EM) wave inside of it with the same EM theory as an optical fiber. Generally, a coaxial cable is formed by an inner conductor, an outer conductor, and the sandwiched insulating layer. In the past decades, the two waveguides, i.e., the optical fiber and the coaxial cable, have developed in two distinct ways, and there are quite a lot of unique technologies and devices of their own. When talking about mechanical strength, coaxial cables are much more robust and can survive a relatively larger strain than optical fibers. Some of the concepts established in fiber optic sensing technologies have been adopted onto coaxial cables due to the fact that the coaxial cables as sensors can provide a solution for some challenging issues (e.g., fragile, bend sensitive, difficult to employ, etc.) faced by their fiber optic counterparts.[17–20] For instance, the Bragg grating has been perfectly implemented on coaxial cables for sensing applications.[17] The idea is to engineer periodical discontinuities on a coaxial cable to form a coaxial cable Bragg grating (CCBG), which has been successfully demonstrated for large strain measurements.[17]

a)Author to whom correspondence should be addressed: jieh@mst.edu

A problem is that the CCBG usually has a long grating length due to the long wavelength of Radio Frequency (RF), which limits its spatial resolution. Very recently, we presented a concept of high-quality factor (Q-factor) coaxial cable Fabry–Pérot resonator (CCFPR) with high measurement resolution, which is believed to be a solution to the spatial resolution problem of CCBG.[21]

So far, most of the developed coaxial cable sensors are used for measurements of various physical parameters such as strain, temperature, crack, and pressure.[17–21] As such, inspired by the optical fiber chemical sensors, there is a need for the development of chemical sensors (such as measurement of liquid dielectric constant) using coaxial cables, and this might address the issues faced by the aforementioned optical fiber-based chemical sensors, such as limited dynamic range, bend sensitive, nonlinear response, fragility, and stringent requirements in fabrication.

In this paper, we report a low-cost and robust homemade hollow coaxial cable Fabry–Pérot resonator (HCC-FPR) for liquid dielectric constant sensing. To the best of our knowledge, this is the first report of using a hollow coaxial cable for chemical sensing applications. In our HCC design, the idea is to use air to replace the traditional insulator. Inspired by the open cavity based fiber FP interferometer sensor, an open cavity is engineered on the HCC. After the cavity is filled with the liquid analyte, an FPR will be formed by the two highly reflective reflectors, i.e., the air-liquid interface and the metal disk. When the HCC-FPR is exposed to surrounding liquids with different dielectric constants, the resonant frequencies of the FPR will shift, thus making the HCC-FPR act as a liquid dielectric constant sensor. In our experiment, we measured the dielectric constant of ethanol/water solutions with various concentrations. Also, monitoring the evaporation of ethanol in ethanol/water mixtures was conducted to demonstrate the capability of the sensor for continuously monitoring the dielectric constant change. The results show that our HCC-FPR sensor has the potential to be a new and low-cost platform for evaporation rate detection. Integrated on a coaxial cable sensing platform, the HCC-FPR is a good sensor head for remotely chemical sensing. Besides, the stringent requirements in fabricating an optical fiber interferometer, such as high manufacturing accuracy, micromachining, can be significantly relieved to construct such an HCC-FPR.

II. SENSOR DESIGN AND MEASUREMENT PRINCIPLE

Figure 1 presents a schematic of the HCC-FPR. The HCC is homemade, which consists of an inner conductor, an outer conductor, and the air in-between served as the dielectric layer. The diameter of the inner conductor is 6 mm; the inner diameter and outer diameter of the outer conductor are 14 mm and 18 mm, respectively. Both the inner and outer conductors are made of stainless steel. A metal disk is welded onto the end of the HCC. The disk shorts the inner and outer conductors, which serves as a highly reflective reflector. An opening groove is engineered on the top of the outer conductor, forming an open cavity and allowing the liquid analyte to enter the cavity freely. A sealing ring is used to prevent the liquid analyte

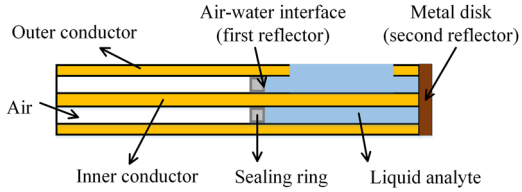

FIG. 1. A schematic drawing of the HCC-FPR for liquid dielectric constant sensing. The HCC consists of an inner conductor, an outer conductor and the air served as the dielectric layer. An FPR is formed by the two highly reflective reflectors, i.e., the air-liquid interface and the metal disk.

from leaking out of the cavity. After filling with the liquid analyte in the open cavity, the air-liquid interface acts as a highly reflective reflector due to large impedance mismatch, together with the metal disk (i.e., a highly reflective reflector), forming an FPR. The HCC-FPR can measure the dielectric constant (ε_r) of the liquid filling in by tracking the shift in the resonant spectra. Compared with an interferometer based sensor such as an FP interferometer, the Q-factor of an FPR sensor is much higher, meaning that the detection limit of an FPR sensor can be improved. It should be noted that if the dielectric constant difference between the air and liquid analyte is not big enough to achieve large impedance mismatch, a highly reflective reflector (e.g., copper reflector[21]) can be engineered on the HCC to serve as the first reflector.

The microwave signal propagating along the HCC is mostly reflected by the first reflector, and the remaining signal with a phase delay passes through and gets to the second reflector. Again, the most energy of the signal gets reflected by the second reflector. Multiple reflections and multiple wave interference occur inside the resonator formed by the two reflectors. The phase delay (δ) between two waves reflected by the first reflector is given by

$$\delta = \frac{4\pi d}{\lambda} = \frac{4\pi f d\sqrt{\varepsilon_r}}{c}, \tag{1}$$

where λ and f are the wavelength and frequency of the EM wave, respectively; d is the resonant cavity length; ε_r is the effective dielectric constant of the liquid analyte; c is the speed of light in vacuum. When the phase delay is equal to $2m\pi$ (m is an integer, i.e., 1, 2, 3, . . .), a resonant pattern can be obtained in the spectrum domain. The resonant frequency (f_{res}) in the reflection spectrum can be written as

$$f_{res} = m\frac{c}{2d\sqrt{\varepsilon_r}}. \tag{2}$$

The spacing between two successive minima of the spectrum, defined as the free spectral range (FSR), can be expressed as

$$FSR = \frac{c}{2d\sqrt{\varepsilon_r}}. \tag{3}$$

When the spectrum shifts due to the change in dielectric constant of the liquid analyte, the resonant frequency shift can be calculated by

$$\Delta f = -f_{res}\frac{1}{2\varepsilon_r}\Delta\varepsilon_r = -\frac{mc}{4d\varepsilon_r^{3/2}}\Delta\varepsilon_r. \tag{4}$$

Thus the dielectric constant change of the liquid analyte in the open cavity of the HCC-FPR can be determined by monitoring

the resonant frequency shift when the cavity length is fixed. From Eq. (4), it concludes that the measurement sensitivity of the liquid dielectric constant ($\Delta f/\Delta\varepsilon_r$) for the developed HCC-FPR is $-mc/4d\varepsilon_r^{3/2}$, which is proportional to the harmonic number m and inversely proportional to the physical cavity length d and the absolute dielectric constant of the liquid analyte ε_r. It should be noted that Eq. (4) is used for the measurement of the change in dielectric constant $\Delta\varepsilon_r$ rather than its absolute value ε_r. The measurement sensitivity of the change in dielectric constant can be considered linear if the change is small. Equation (3) is used for the measurement of the absolute value of the liquid dielectric constant by acquiring the *FSR* from the recorded reflection spectrum, where the physical cavity length d and the speed of light in vacuum c are both mathematical constants. According to Eq. (2), the thermal expansion of the cavity length could lead to a resonant frequency shift, leading to a temperature cross talk. The temperature sensitivity can be calculated to be $-mc\alpha_{CTE}/2d\sqrt{\varepsilon_r}$, where α_{CTE} is the coefficient of thermal expansion of stainless steel. Thus, the dielectric constant-temperature cross-sensitivity can be determined by $2\varepsilon_r\alpha_{CTE}$. In field applications, a thermocouple needs to be used for temperature compensation.

III. EXPERIMENTAL RESULTS AND DISCUSSIONS

The experimental setup for using the HCC-FPR to measure liquid dielectric constant is schematically illustrated in Fig. 2(a). An FPR was engineered on a homemade HCC, which was designed to be connected to a commercial coaxial cable (e.g., RG-58/U) via an SMA (SubMiniature version A) to N adapter. A vector network analyzer (VNA, Agilent 8753ES) was employed to acquire the amplitude reflection spectrum (S(1, 1)) of the HCC-FPR. The liquid analyte was stored in a glass container. The VNA was set to measure the frequency response over a range between 100 kHz and 1.2 GHz. The sampling points and the intermediate frequency bandwidth (IFBW) were configured to be 1601 and 300 Hz. Data recording and processing were accomplished by a personal computer (PC) connected to the VNA. A photograph of our HCC-FPR sensor is presented in Fig. 2(b). The open cavity length of the FPR is around 4.60 cm.

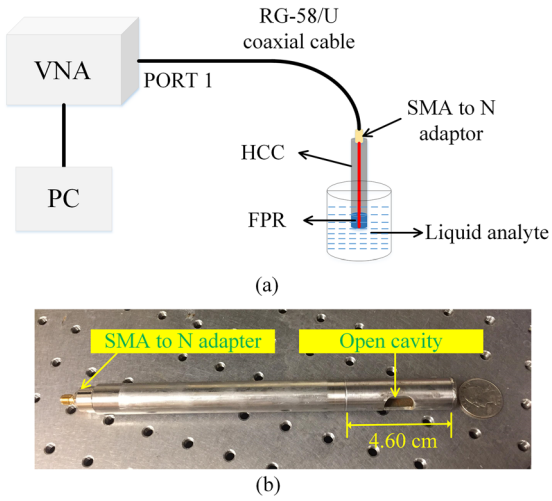

FIG. 2. (a) A schematic of the experimental setup. A vector network analyzer (VNA, Agilent 8753ES) was employed to acquire S(1, 1) of the HCC-FPR. The hollow coaxial cable was connected to the port 1 through an RG-58/U coaxial cable. The FPR was immersed in the liquid analyte when measuring the liquid dielectric constant. (b) A photograph of the HCC-FPR sensor. The length of the open cavity is 4.60 cm.

The HCC-FPR was first tested with dry air and tap water filling in the cavity in a clean room at room temperature, respectively. Figure 3 plots the amplitude reflection spectra (S(1, 1)) of the HCC-FPR under two different conditions. It is quite clear that a resonant pattern was obtained after the open cavity was filled with water. Three resonant valleys in the HCC-FPR spectrum filled with water can be clearly identified with a good contrast of 10 dB, indicating a high quality microwave resonator was formed by the two highly reflective reflectors due to impedance mismatch, i.e., the air-water interface and the metal disk as expected. The *FSR* of the resonant pattern was calculated to be 368.172 MHz. According to Eq. (3), the dielectric constant of the tap water filled in the cavity was calculated to be 78.44 around 0.2 GHz giving by the physical length of the cavity to be 4.60 cm. The Q-factors of the three valleys, which are mathematically defined by the ratio of the center frequency to the full width at half maximum, are calculated to be 16, 33, and 23, respectively. The large Q-factors indicate that the HCC-FPR is a resonance device rather than an interferometric device (e.g., an FP interferometer with a Q-factor of 2).

To characterize the dielectric constant response of the HCC-FPR, the sensor head was fully immersed in ethanol/water solutions with different ε_r in a clean room at a constant temperature of 20 °C (±1 °C). The ε_r was modified by changing the ethanol mass ratio of ethanol/water solutions.[22] Figure 4 plots a dip in reflection spectra as the ethanol concentration increases. The dip frequency shifted to the higher frequency region, revealing the dielectric constant of the solutions decreased as the ethanol concentration increased. Since ε_r of the water at RF ranges ($\varepsilon_r \sim 80.37$) is greater than that of the ethanol ($\varepsilon_r \sim 25.07$), it is expected that the effective dielectric constant of the water/ethanol mixtures decreases with the increment of the ethanol concentration. From Fig. 4, it can also be observed that the contrast of the resonant valley increases as

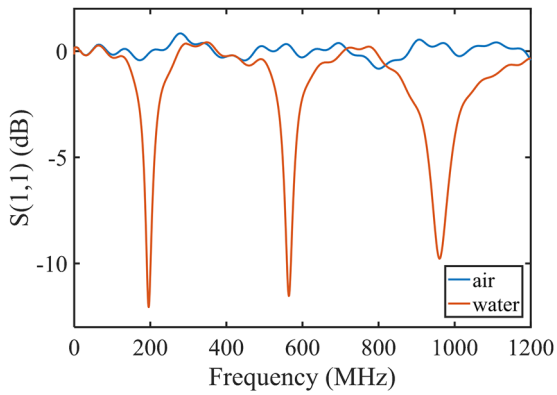

FIG. 3. Amplitude reflection spectra of the HCC-FPR before and after filling in the open cavity with tap water. A resonant pattern could be obtained after the cavity was filled with water, meaning that an FPR was formed by the air-water interface and the metal disk due to large impedance mismatch.

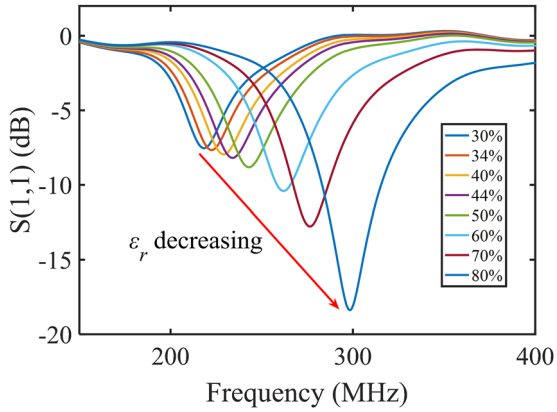

FIG. 4. The change in reflection spectra with respect to ethanol concentration in the ethanol/water solution. The dip frequency shifted to higher frequency region as the ethanol mass concentration increases from 30% to 80%.

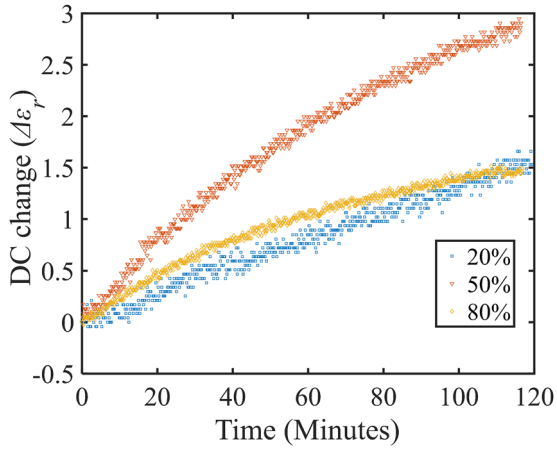

FIG. 6. Measured dielectric constant (DC) change of ethanol/water mixtures with different ethanol concentration (i.e., 20%, 50%, and 80%) as a function of time.

the ethanol concentration increases. This is because the attenuation of the RF waves propagating in the HCC decreases as ethanol concentration increases.

Figure 5 plots the change in fundamental resonance frequency with respect to the dielectric constant of the ethanol/water solution. It can be seen that the relationship is slightly nonlinear, and the slope or sensitivity decreases as the dielectric constant increases, which is consistent with Eq. (4) where the slope is inversely proportional to the absolute dielectric constant of the liquid analyte. To evaluate the stability of the HCC-FPR, the dielectric constant was measured as a function of time when the open cavity was filled with tap water. The inset of Fig. 5 shows the deviation of the dielectric constant (DC) measured every 10 s for 30 min. The standard deviation of the measured data was found to be 0.0087, corresponding to a relative measurement resolution of 1×10^{-4}.

The ability of the HCC-FPR sensor for continuously monitoring the evaporation of ethanol/water mixtures with different ethanol volume concentrations (i.e., 20%, 50%, and 80%) was also demonstrated at room temperature. In the experiment, the VNA was controlled by a PC to record the resonant reflection spectra every 11 s for 2 h. Figure 6 presents the dielectric constant change as a function of time for various ethanol volume concentrations. It can be found that the dielectric constant of the mixtures increased over time. This is because that in this case, ethanol, being more volatile than water, preferentially left the ethanol/water mixtures, resulting in a decrease in ethanol content. As shown in Fig. 6, the dielectric constant change rate of the mixture with 50% ethanol was faster than those of the mixtures with 20% and 80% ethanol, meaning that the concentration change rate of the mixture with 50% ethanol was faster than those of the other two. Interestingly, there was little difference in the dielectric constant change rate of the 20% and 80% solutions. It is possible that the evaporation rates of water and ethanol are different under different compositions. In our future work, the detailed and quantitative investigation will be done by using such an HCC-FPR. It should be noted that the update rate of the reflection spectra can be as high as several hundred hertz so that real-time dynamic monitoring can be achieved for the proposed HCC-FPR device. Therefore, the HCC-FPR has the potential to be a new and low-cost platform for evaporation rate detection with high performance, which may play a significant role in chemical engineering society.[23]

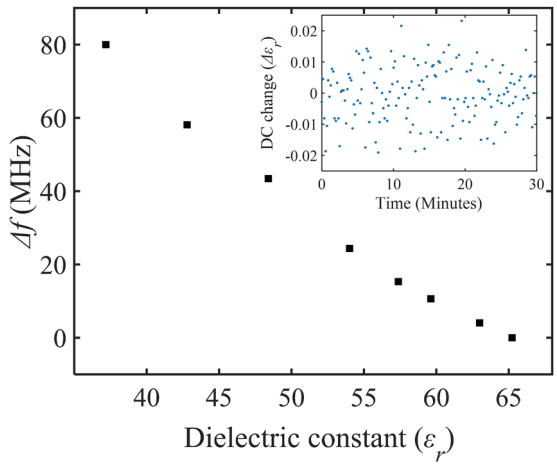

FIG. 5. Resonant frequency change with respect to dielectric constant. Inset: Plot of the measured dielectric constant change as a function of time.

IV. CONCLUSION

To summarize, we propose and demonstrate a low-cost and robust homemade HCC-FPR sensor for liquid dielectric constant measurements. In the HCC design, the traditional insulating layer between the inner conductor and outer conductor is replaced by air. A metal disk was welded onto the end of the HCC serving as a highly reflective reflector. An opening groove was engineered on the top of the outer conductor near the metal disk to form an open cavity. When the open cavity is exposed to the liquid analyte (e.g., water), an FPR will be constructed with two highly reflective reflectors, i.e., the air-water interface and the metal disk. The resonant frequency shifts with the dielectric constant variations of the liquid analyte filling in the open cavity. The HCC-FPR was demonstrated for measurements of the dielectric constant of the ethanol/water solutions with different ethanol

concentrations. Monitoring the evaporation of ethanol in ethanol/water solutions was also conducted to verify its ability for continuously monitoring dielectric constant change. The experimental results showed that the HCC-FPR sensor has the potential to be a new platform for evaporation rate detection. More importantly, the unique accessible FP open cavity makes it attractive for sensing applications in the various fields. The concept of the HCC-FPR chemical sensor was inspired by its optical counterpart, optical fiber based FP interferometer family. As a result, it inherits the advantages of optical fiber sensors, such as high measurement resolution, high sensitivity, remote operation, and multiplexing capability. Meanwhile, by monitoring the resonant spectrum in RF domain, the HCC-FPR offers great advantages that are incomparable by conventional optical fiber sensors, including ease of fabrication, robustness, large dynamic range, bending resistance, and potentially low cost in signal interrogation.

ACKNOWLEDGMENTS

The work was supported by University of Missouri Research Board.

[1]O. Wolfbeis, "Fiber-optic chemical sensors and biosensors," Anal. Chem. **76**, 3269–3284 (2004).
[2]Z. Chen, L. Yuan, G. Hefferman, and T. Wei, "Ultraweak intrinsic Fabry–Perot cavity array for distributed sensing," Opt. Lett. **40**, 320–323 (2015).
[3]Y. Chen, Q. Han, T. Liu, and X. Lü, "Self-temperature-compensative refractometer based on singlemode–multimode–singlemode fiber structure," Sens. Actuators, B **212**, 107–111 (2015).
[4]Q. Han, X. Lan, J. Huang, A. Kaur, T. Wei, Z. Gao, and H. Xiao, "Long-period grating inscribed on concatenated double-clad and single-clad fiber for simultaneous measurement of temperature and refractive index," IEEE Photonics Technol. Lett. **24**, 1130–1132 (2012).
[5]Y. Huang, T. Wei, Z. Zhou, Y. Zhang, G. Chen, and H. Xiao, "An extrinsic Fabry–Perot interferometer-based large strain sensor with high resolution," Meas. Sci. Technol. **21**, 105308 (2010).
[6]H. J. Patrick, A. D. Kersey, and F. Bucholtz, "Analysis of the response of long period fiber gratings to external index of refraction," J. Lightwave Technol. **16**(9), 1606 (1998).
[7]I. M. Ishaq, A. Quintela, S. W. James, G. J. Ashwell, J. M. Lopez-Higuera, and R. P. Tatam, "Modification of the refractive index response of long period gratings using thin film overlays," Sens. Actuators, B **107**(2), 738–741 (2005).
[8]W. Liang, Y. Huang, Y. Xu, R. K. Lee, and A. Yariv, "Highly sensitive fiber Bragg grating refractive index sensors," Appl. Phys. Lett. **86**(15), 151122 (2005).
[9]H. Meng, W. Shen, G. Zhang, C. Tan, and X. Huang, "Fiber Bragg grating-based fiber sensor for simultaneous measurement of refractive index and temperature," Sens. Actuators, B **150**(1), 226–229 (2010).
[10]A. Iadicicco, S. Campopiano, A. Cutolo, M. Giordano, and A. Cusano, "Self temperature referenced refractive index sensor by non-uniform thinned fiber Bragg gratings," Sens. Actuators, B **120**(1), 231–237 (2006).
[11]R. C. Jorgenson and S. S. Yee, "A fiber-optic chemical sensor based on surface plasmon resonance," Sens. Actuators, B **12**(3), 213–220 (1993).
[12]M. H. David and J. Villatoro, "High-resolution refractive index sensing by means of a multiple-peak surface plasmon resonance optical fiber sensor," Sens. Actuators, B **115**(1), 227–231 (2006).
[13]Y. Du, S. Jothibasu, Y. Zhuang, C. Zhu, and J. Huang, "Rayleigh backscattering based macrobending single mode fiber for distributed refractive index sensing," Sens. Actuators, B **248**, 346–350 (2017).
[14]Y. Zhao, X. Liu, R. Q. Lv, and Q. Wang, "Simultaneous measurement of RI and temperature based on the combination of Sagnac loop mirror and balloon-like interferometer," Sens. Actuators, B **243**, 800–805 (2017).
[15]T. Wei, Y. Han, Y. Li, H. L. Tsai, and H. Xiao, "Temperature-insensitive miniaturized fiber inline Fabry-Perot interferometer for highly sensitive refractive index measurement," Opt. Express **16**(8), 5764–5769 (2008).
[16]J. Tian, Z. Lu, M. Quan, Y. Jiao, and Y. Yao, "Fast response Fabry–Perot interferometer microfluidic refractive index fiber sensor based on concave-core photonic crystal fiber," Opt. Express **24**(18), 20132–20142 (2016).
[17]T. Wei, S. Wu, J. Huang, H. Xiao, and J. Fan, "Coaxial cable Bragg grating," Appl. Phys. Lett. **99**(11), 113517 (2011).
[18]J. Huang, T. Wang, L. Hua, J. Fan, H. Xiao, and M. Luo, "A coaxial cable Fabry-Perot interferometer for sensing applications," Sensors **13**(11), 15252–15260 (2013).
[19]J. Huang, X. Lan, W. Zhu, B. Cheng, J. Fan, Z. Zhou, and H. Xiao, "Interferogram reconstruction of cascaded coaxial cable Fabry-Perot interferometers for distributed sensing application," IEEE Sens. J. **16**(11), 4495–4500 (2016).
[20]B. Cheng, L. Yuan, W. Zhu, Y. Song, and H. B. Xiao, "A coaxial cable magnetic field sensor based on ferrofluid filled Fabry-Perot interferometer structure," Sens. Actuators, A **257**, 194–197 (2017).
[21]M. F. Ahmed, T. Xue, B. Wu, and J. Huang, "High quality factor coaxial cable Fabry-Perot resonator for sensing applications," IEEE Sens. J. **17**(10), 3052–3057 (2017).
[22]J. Wyman, "The dielectric constant of mixtures of ethyl alcohol and water from-5 to 40," J. Am. Chem. Soc. **53**(9), 3292–3301 (1931).
[23]P. Innocenzi, L. Malfatti, S. Costacurta, T. Kidchob, M. Piccinini, and A. Marcelli, "Evaporation of ethanol and ethanol–water mixtures studied by time-resolved infrared spectroscopy," J. Phys. Chem. **112**(29), 6512–6516 (2008).